Artificial muscles for a novel simulator in minimally invasive spine surgery*

Marianne Hollensteiner[1], David Fuerst[1,2] and Andreas Schrempf[1]

***Abstract*—Vertebroplasty and kyphoplasty are commonly used minimally invasive methods to treat vertebral compression fractures. Novice surgeons gather surgical skills in different ways, mainly by "learning by doing" or training on models, specimens or simulators. Currently, a new training modality, an augmented reality simulator for minimally invasive spine surgeries, is going to be developed. An important step in investigating this simulator is the accurate establishment of artificial tissues. Especially vertebrae and muscles, reproducing a comparable haptical feedback during tool insertion, are necessary. Two artificial tissues were developed to imitate natural muscle tissue. The axial insertion force was used as validation parameter. It appropriates the mechanical properties of artificial and natural muscles. Validation was performed on insertion measurement data from fifteen artificial muscle tissues compared to human muscles measurement data. Based on the resulting forces during needle insertion into human muscles, a suitable material composition for manufacturing artificial muscles was found.**

***Index Terms*—patient simulator, vertebro-/kyphoplasty, needle insertion force, artificial soft tissues**

I. INTRODUCTION

As the population in industrial countries grows older and older, osteoporosis and further osteoporotic vertebral compression fractures (VCFs) seem to get an enormous clinical problem [1], [2]. But, VCFs also occur in the wake of malign bone tumors or osteomyelitis [2]. Each year about 1.4 million VCFs occur in Europe and about seven hundred thousand in the US, respectively [3]. Mostly, VCFs are accompanied by pain, loss of height, kyphosis, numbness, weakness or tingling because of clamped or damaged conducting nerves [4]. Beneath conventional treatment, including rest, bracing and administration of analgesics, the most common surgical treatments for VCFs are cement augmentation techniques. Kyphoplasty and vertebroplasty are showing good results in achieving pain relief [2], [5], [6] and avoid the adverse effects of pharmacological treatments [4]. Both techniques are performed percutaneously, stabilizing the fractured vertebra internally by an injection of bone cement [6]. The gathering of surgical skills currently is carried out in traditional or simulated environments. Training is either performed by a) "learning by doing" on the patient him- or herself, b) computer based models, c) studies on animal or human specimen and d) patient simulators [5], [7]. Normally, the medical education is done as immersion experience in a clinical environment which can be a high risk for the patient [7]. As a new training modality and to improve patient safety in the future, a novel patient simulator is currently going to be developed [8]. For a realistic haptic feedback, an augmented reality (AR) simulator consisting of a patient phantom and a tool tracking system was designed (see Fig 1). Novel surgeons will be able to train the needle insertion on artificial tissues. Integral parts of this simulator are these synthetic tissues, which should generate a high fidelity haptic feedback for surgical needle insertion and therefore should have assimilable mechanical properties to natural tissues. Suitable artificial vertebrae were already developed and validated [9], [10]. The aim of this study was to find materials which provide a feedback comparable to natural muscles and skin.

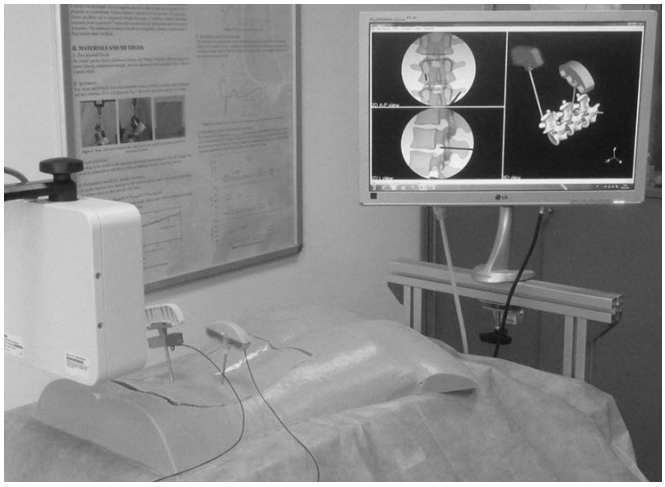

Fig 1: AR simulator for cement augmentation techniques (magnetic tracking system, surgical needles, patient phantom and virtual fluoroscopic projection)

II. MATERIALS AND METHODS

An earlier study identified the axial insertion force as main parameter to develop artificial tissues [9]. To manufacture human artificial muscles, the axial insertion force of an vertebroplasty tool, driven robotically, was used. To work out the characteristics of axial force against time, insertion force measurements on specimens were performed. Tests on human muscle tissues were carried out either, to test comparability of artificial muscles. With the results of these measurements,

*This work was supported by funds from the INTERREG program "Bavaria-Austria" for the project "PatientSim" (project number J00335).

[1]Department of Medical Device Engineering, Upper Austria University of Applied Sciences, School of Applied Health and Social Sciences, Garnisonstraße 21, 4020 Linz, Austria.

[2]Paracelsus Medical University, Strubergasse 21, 5020 Salzburg, Austria.

an artificial muscle made of silicone was developed and validated by means of a parametrical model.

A. Insertion measurement test setting

For all insertion tests, an eleven gauge diamond tip needle (Kyphon Inc., KyphX Osteo Introducer, Sunnyvale, CA) was used. The insertion measurements were performed in three phases (see Fig 2). During insertion phase the needle was inserted into the specimens for an insertion depth of $20\,mm$ with a feed rate of $10\,mm/s$ (phase 1=insertion). In the relaxation phase the needle was stopped for eight seconds (phase 2=relaxation). Then the needle was removed with a feed rate of $10\,mm/s$ during the extraction phase (phase 3=extraction). This procedure was chosen to mirror a typical manner of soft tissue measurements to observe its relaxation [11]. The insertion measurements were performed with a self

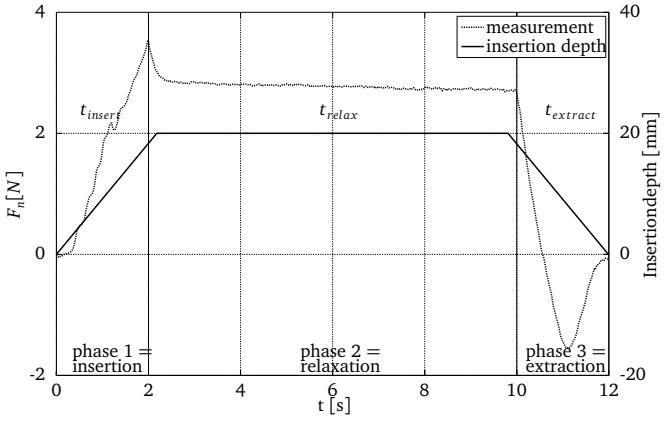

Fig 2: Insertion depth/ force/ time curve and explanation of measurement phases: insertion, relaxation and extraction

constructed uni-axial material testing machine consisting of a linear actuator connected to a $500\,N$ load cell.

B. Human specimen

One fresh frozen spine, consisting of vertebrae and sufficient surrounding soft tissues, was used as specimen. The vertebrae were left within the testing sample to preserve muscles tension, measuring insertion into muscle tissue covered by skin and tendons. For fixation, the spines were fixed to the material testing machine with clamps.

C. Artificial muscle tissue blocks

To create artificial back muscles with comparable haptic feedback, a silicone rubber was chosen as basic material. Two different silicone oils were added to the silicone rubber in amounts of 10 to 70 (in intervals of ten) percent of the whole rubber mass (further named as silicone block 1 "SB1" and silicone block 2 "SB2") as lubricants. To imitate fasciae, special cling films were embedded in a depth of approximately $10\,mm$ in selected silicone blocks. The mixtures were molded for four hours. Further, selected mixtures were also fused with red color additive to provide also a visual impression of muscle tissue.

D. Parametrical model for needle insertion

In order to derive characteristical parameters for needle-tissue interaction, a parametrical model was developed. The tissue is modeled by a standard linear solid model which yields the tissue force $F_t(t)$. The interaction between needle and tissue is given by the needle force $F_n(t)$. The needle position $x_n(t)$ as well as the needle speed $v_t(t)$ are imposed from the insertion experiment (see Fig 2) . The deformation of the tissue is given by $x_t(t)$ with the corresponding insertion speed $v_t(t)$. With the legit insertion depth $\Delta x(t) = x_n(t) - x_t(t)$ and insertion speed $\Delta v(t) = v_n(t) - v_t(t)$, the mathematical model for needle insertion is given by

$$\frac{d\Delta x(t)}{dt} = \Delta v(t) \quad (1)$$

$$\frac{d\Delta v(t)}{dt} = \frac{1}{m_t}(F_n(t) - F_t(t)), \quad (2)$$

where m_t accounts for the tissue mass, which is moved due to tissue deformation. The tissue force $F_t(t)$ is obtained from a standard linear solid model (spring $c_1$in parallel with a Maxwell model with spring c_2 and dashpot d)

$$\frac{dF_t(t)}{dt} = -\frac{c_2}{d}F_t(t) + \frac{c_1 c_2}{d}(x_n(t) - \Delta x(t)) + (c_1 + c_2)(v_n(t) - \Delta v(t)). \quad (3)$$

The needle force $F_n(t)$ is composed by cutting and clamping forces (see [10] for bone tissue) and is modeled by

$$F_n(t) = \begin{cases} f_{cut} \cdot \lambda(\Delta x(t)) \cdot \Delta x(t) & \text{insertion \& relax. phase} \\ F_{t,ex}(t) & \text{extraction phase} \end{cases}$$

During insertion and relaxation phase ($v_n \geq 0$) the needle force increases with insertion depth Δx. The corresponding proportional cutting coefficient is given by f_{cut}. Hereby the needle geometry plays an important role, which is considered by a depth-dependent shape function $\lambda(\Delta x)$. During extraction phase ($v_n < 0$) a conjoint movement of needle and tissue emerges, until a certain force threshold F_{rel} is exceeded and the needle slips out of the tissue (see Fig 3 (a)). The needle force for the conjoint movement $F_{t,ex}(t)$ is obtained from Eq (3) where $\Delta x(t) = \Delta\bar{x} = const.$ and $\Delta v(t) = 0$.

III. RESULTS

Over all insertion measurements, the typical trajectory of soft tissue insertion measurements could be identified. In the descent phase, an exponential like rise of the measured force, followed by sharp ruptures and again rising slopes, were observed. As a consequence of muscle elasticity, the maximum peak is proportional to the depth inserted into (phase 1=insertion). During tissue relaxation (phase 2=relaxation), repulsion forces are acting on the needle, mainly depending on the needle's tip. While the needle was removed, only friction forces were acting. During extraction the tissue moved conjointly with the needle (phase 3=extraction) until a certain threshold (negative forces in Fig 3 (a)) was exceeded and the needle slipped out of the tissue [12].

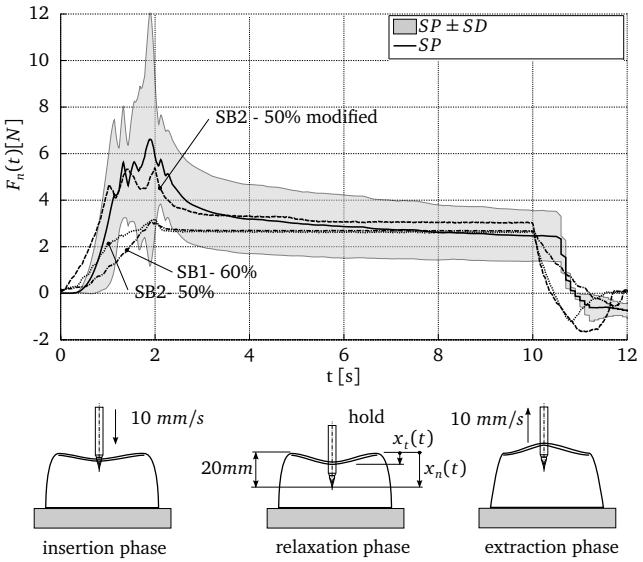

(a) Mean plots for insertion measurement (SP - mean value for human specimen, SD - standard deviation (gray area), 50% SB2 modified - silicone rubber mixture 2 with 50% silicone oil, red color additive and artificial fascia).

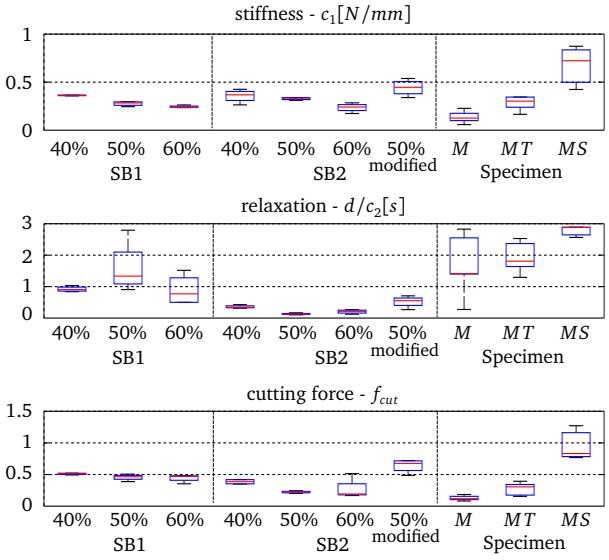

(b) Characteristic model parameters (SB - silicone block mixtures, M - muscle tissue, MT - muscle tissue covered with tendon, MS - muscle tissue covered with skin)

Fig 3: Comparison of artificial tissue and human specimen.

A. Human specimen

The average force of the needle insertion measurements into the human muscle and the corresponding standard deviation (SD) are shown in Fig 3 (a). The human specimen average (SP) is drawn as a bold, solid line. The positive and negative standard deviations are depicted as thin, solid lines, filled by a gray area. Different parts of the human muscles have been measured and therefore, a wide spread between the measured forces has been observed. This is due to the fact, that biomechanical parameters of muscles vary between claimed parts of a muscle. The measurement curves clearly showed the peaks according to the three measurement phases. During the insertion phase, small extra peaks were recorded. These extra peaks occurred because of the punction of fasciae, which show higher puncture forces than the muscle. The average needle forces of the measurement into the human muscle are $6.66\,N$ for the maximum insertion force, $2.48\,N$ for the relaxation and $-0.57\,N$ for the maximum extraction force.

B. Artificial muscle blocks

In Fig 3 (a), the results of the three best fitting silicone blocks are illustrated. The average curves of four insertion measurements on each of the blocks are plotted. The single insertions into the silicone block with same amount of oils only varied slightly which may be caused by an inhomogeneous mixing of the silicone components and the oils. Their values for maximum insertion, relaxation and extraction force varied due to the amounts of silicone oil added. Concerning the different portions of silicone oils, the resulting forces showed different slopes, especially during insertion phase. With increasing quantity of oil, the friction between tool and silicone dropped and the insertion forces became smaller. For the SB1 blocks, the maximum insertion force peaks varied from $7.67\,N$ to $2.68\,N$, the relaxation forces from $6.51\,N$ to $2.25\,N$ and the maximum extraction forces from $-2.45\,N$ to $-0.43\,N$. In case of SB2, they ranged from $7.66\,N$ to $2.82\,N$, $6.25\,N$ to $1.66\,N$ and from $-2.63\,N$ to $-0.45\,N$.

C. Parametrical model for needle insertion

The parametrical model for the needle-tissue interaction, Eq (1) - (3), was fitted to the data (see Fig 4) with a mean relative error of 2.02% and an overall maximum error of 4.47%. The characteristical parameters c_1, d/c_2 and f_{cut} were computed for all insertion measurements which led to box-plots depicted in Fig 3 (b). Obviously, the spring

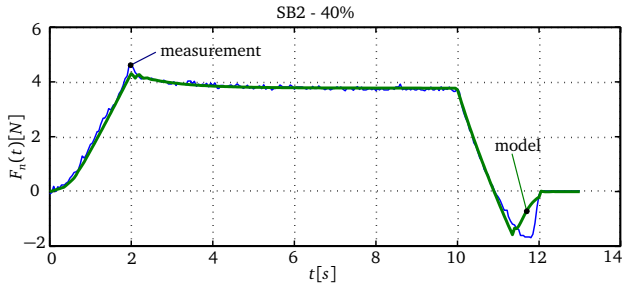

Fig 4: Parametrical model compared to measurement for SB2 with 40% silicone oil

constant c_1, which mainly determines the equilibrium force after relaxation decreases for an increased amount of silicone

oil. A similar behavior is observed for parameter f_{cut}, responsible for cutting forces. The speed of relaxation is determined by time constant $\tau = d/c_2$, which increases for higher amounts of silicone oil. Compared to human specimen, the relaxation time constants are shorter for all artificial tissue blocks. With respect to relaxation, the artificial tissue is only able to provide a rough approximation of human tissue. There, the relaxation behavior is mainly influenced by a significant amount of free fluid, which redistributes after insertion. Silicone oil added to the artificial tissue blocks allows to control the viscosity and hence the relaxation time constant τ. However, the oil is bonded and cannot move freely. The boxes of SB1 better fit the relaxation d/c_2 of human muscle whereas the SB2-50% box best fit the cutting force f_{cut}. For the stiffness c_1 all measured blocks provide acceptable results (see Fig 3 (b)).

IV. DISCUSSION

Haptic feedback is a combination of tactile and kinesthetic feedback, perceived by tactile skin receptors and sensory receptors in joints, muscles and tendons [13]. It is excessively important in open and minimal invasive surgery to sense or "feel" different tissues. It is nearly as important as the visual feedback during a surgery [14]. According to [13], training on simulators with haptic feedback transfers skills to novel surgeons significantly compared to training without haptical feedback. The degree of realism of a surgical simulator depends on the capabilities of the simulator, either hard- or software. The more realistic, the better the training environment, the better the transfer of skills [15]. Further, a simulated environment is less risky for the patient and even less stressful for a novice surgeon, than training on patients directly in an operating room [16]. A surgeon should be able to identify and to handle different tissues, so the image-guided surgery's disadvantage is the decrease of haptic feedback to the surgeon. A solution to either acquire operating room techniques and also get ideas of haptic feedback are AR simulators. But, it is difficult to reproduce realistic and real-time deforming soft tissues [17]. This study therefore was focused on the development of artificial muscle tissues for an AR simulator for minimally invasvie spine surgeries, especially. The parametric model identifies the silicone blocks SB2-50% and the SB1-60% as the most suitable natural muscle imitating materials, especially for the relaxation and cutting forces. By adding the red color additive and a special cling film into the SB2-50% block, the insertion force increased and the measurement curve almost coincide with the human muscle average (Fig. (3) (a) - SB2-50% modified). This modified block fits best to provide an appropriate haptical as well as a visual feedback. The mainly pierced muscle during vertebro- and kyphoplasty is the musculus erector spinae (MES). In a neutral position the MES boasts a diameter of $34.5 \pm 4.1\,mm$ [18]. For the usage of the silicone-oil mixtures in the currently developed patient simulator, blocks with a thickness of $50\,mm$ were molded and artificial vertebrae were embedded into it, so the path from inserting the needle into the artificial tissue to reach the bony structures of the vertebrae is approximately $35\,mm$. The SB2 mixtures were more easily to blend and mold and the SB1 mixtures showed an oozing of the silicone oil. Hence a change of the mechanical properties over time was visible. Because of these reasons the modified SB2-50% mixture with the red additive was chosen to be used in the patient simulator.

REFERENCES

[1] N. E. Lane. Epidemiology, etiology, and diagnosis of osteoporosis. *American Journal of Obstetrics and Gynecology*, 194(2, Supplement):S3 – S11, 2006.

[2] J. Y. Lee, M. R. Lim, S. C. Ludwig, I. Elias, T. R. Kuklo, and Vaccaro A. R. Vertebroplasty and kyphoplasty for vertebral compression fractures. *Seminars in Spine Surgery*, 17(3):158 – 164, 2005.

[3] EPOS Group, D. Felsenberg, et al. Incidence of vertebral fracture in europe: results from the european prospective osteoporosis study (epos). *J Bone Miner Res*, 17(4):716–724, Apr 2002.

[4] R. Vallejo and R. M. Benyamin. Vertebral augmentation techniques for the treatment of vertebral compression fractures: A review. *Techniques in Regional Anesthesia and Pain Management*, 14:133–141, 2010.

[5] Adam Dubrowski, Ryan Brydges, Lisa Satterthwaite, George Xeroulis, and Roger Classen. Do not teach me while i am working! *Am J Surg*, 203(2):253–257, Feb 2012.

[6] S. R. Garfin and M. A. Reilley. Minimally invasive treatment of osteoporotic vertebral body compression fractures. *Spine J*, 2(1):76–80, 2002.

[7] Gary B. Nackman, Mordechai Bermann, and Jeffrey Hammond. Effective use of human simulators in surgical education. *J Surg Res*, 115(2):214–218, Dec 2003.

[8] D. Fuerst and A. Schrempf. Patientsim - development of an augmented reality simulator for surgical training of vertebroplasty and kyphoplasty. In *9-th IASTED International Conference on Biomedical Engineering*, 2012.

[9] D. Fuerst, D. Stephan, P. Augat, and A. Schrempf. Foam phantom development for artificial vertebrae used for surgical training. *Conf Proc IEEE Eng Med Biol Soc*, 2012:5773–5776, 2012.

[10] M. Hollensteiner, D. Fuerst, and A. Schrempf. Artificial vertebrae for a novel simulator in minimally invasive spine surgery. *Biomed Tech (Berl)*, Sep 2013.

[11] N. Abolhassani, R. Patel, and M. Moallem. Needle insertion into soft tissue: a survey. *Med Eng Phys*, 29(4):413–431, May 2007.

[12] B. Maurin, L. Barbe, B. Bayle, P. Zanne, J. Gangloff, M. de Mathelin, A. Gangi, L. Soler, and A. Forgione. In vivo study of forces during needle insertions. *Proceedings of the scientific workshop on medical robotics, navigation and visualization*, pages 415–422, 2004.

[13] R. Aggarwal, K. Moorthy, and A. Darzi. Laparoscopic skills training and assessment. *British Journal of Surgery*, 91(12):1549–1558, Dec 2004.

[14] G. Picod, A. C. Jambon, D. Vinatier, and P. Dubois. What can the operator actually feel when performing a laparoscopy? *Surgical Endoscopy*, 19(1):95–100, Jan 2005.

[15] K. S. Lehmann, J. P. Ritz, H. Maass, H. K. Cakmak, U. G. Kuehnapfel, C. T. Germer, G. Bretthauer, and H. J. Buhr. A prospective randomized study to test the transfer of basic psychomotor skills from virtual reality to physical reality in a comparable training setting. *Annals of Surgery*, 241(3):442–449, Mar 2005.

[16] K. Moorthy, Y. Munz, S. K. Sarker, and A. Darzi. Objective assessment of technical skills in surgery. *BMJ*, 327(7422):1032–1037, Nov 2003.

[17] P. Stroem, L. Hedman, L. Saerna, A. Kjellin, T. Wredmark, and L. Fellaender-Tsai. Early exposure to haptic feedback enhances performance in surgical simulator training: a prospective randomized crossover study in surgical residents. *Surgical Endoscopy And Other Interventional Techniques*, 20(9):1383–1388, 2006.

[18] T. Masuda, K. Miyamoto, K. Oguri, T. Matsuoka, and K. Shimizu. Relationship between the thickness and hemodynamics of the erector spinae muscles in various lumbar curvatures. *Clinical Biomechanics*, 20(3):247 – 253, 2005.